

Open Research Online

The Open University's repository of research publications and other research outputs

A comparative study of proton radiation damage in p- and n-channel

Conference or Workshop Item

How to cite:

Gow, J.; Murray, N. J.; Holland, A. D.; Burt, D. and Pool, P. (2009). A comparative study of proton radiation damage in p- and n-channel. In: Proceedings of SPIE: UV, X-Ray, and Gamma-Ray Space Instrumentation for Astronomy XVI, 3 Aug 2009, San Diego, USA.

For guidance on citations see [FAQs](#).

© SPIE - The International Society for Optical Engineering

Version: Accepted Manuscript

Link(s) to article on publisher's website:
<http://dx.doi.org/doi:10.1117/12.826866>

Copyright and Moral Rights for the articles on this site are retained by the individual authors and/or other copyright owners. For more information on Open Research Online's data [policy](#) on reuse of materials please consult the policies page.

oro.open.ac.uk

A Comparative Study of Proton Radiation Damage in p- and n-Channel CCDs

J. Gow^{*a}, N. J. Murray^a, A. D. Holland^a, D. Burt^b, P. Pool^b

^ae2v centre for electronic imaging, The Open University, PSSRI, Milton Keynes, MK7 6AA, UK

^be2v technologies plc, 106 Waterhouse Lance, Chelmsford, Essex, CM1 2QU, UK

ABSTRACT

It has been demonstrated that p-channel charge coupled devices (CCDs) are more radiation hard than conventional n-channel devices as they are not affected by the dominant electron trapping caused by the displacement damage defect the E-centre (phosphorus-vacancy). This paper presents a summary of the results from a comparative study of n-channel and p-channel CCDs each type operated under the same conditions. The CCD tested is the e2v technologies plc CCD47-20, a 1024×1024 frame transfer device with a split output register, fabricated using the same mask to form n-channel and p-channel devices. The p-channel devices were irradiated to a 10 MeV equivalent proton fluence of 4.07×10^{10} protons.cm⁻² and 1.35×10^{11} protons.cm⁻², an n-channel CCD was irradiated to a 10 MeV equivalent proton fluence of 1.68×10^9 protons.cm⁻², however due to time constraints the n-channel device was not characterised, n-channel comparisons are instead made using a CCD02. As expected the p-channel CCD demonstrated improved radiation tolerance when compared to the n-channel CCD, at -90 °C there is an approximate $\times 7$ and $\times 15$ improvement in tolerance to radiation induced parallel and serial CTI respectively for equivalent pixel geometries.

Keywords: CCD, Proton radiation damage, p-channel, n-channel, charge transfer efficiency, displacement damage hardened

1. INTRODUCTION

The work presented in this paper has been carried by the e2v centre for electronic imaging at the Open University to investigate the post proton irradiation performance of n-channel and p-channel CCDs fabricated using the same mask set. It is essential for a space mission that the selected detector meets the performance requirements over the mission duration, accounting for performance loss due to the space radiation environment [1]. Displacement damage caused by protons within the Earth's radiation belts and from cosmic rays (solar and galactic) generate stable lattice defects within the silicon, creating energy levels within the silicon band-gap. The three main stable defects, for n-channel CCDs, are the phosphorous vacancy (E-centre) at 0.44 eV, the oxygen-vacancy (A-centre) at 0.18 eV (both as a result of impurity atoms within the lattice), and the divacancy (J-centre) at 0.40 eV and 0.25 eV consisting of two adjacent vacancies. The E-centre is located at near mid-gap, the ideal location for electron trapping. An n-channel device uses phosphorus as the dopant atom for the buried channel; it was suggested and demonstrated that using boron to create a p-channel device would reduce the post irradiation increase in charge transfer inefficiency (CTI) [2].

It is difficult to compare CTI results taken using different operating conditions and equipment setups, as described elsewhere in this volume [3]. The aim of this work was to provide a definitive comparison of n-channel and p-channel devices. The devices were to be operated using the same drive voltages and timings, held in the same position within the test facility and exposed to the same incident X-ray flux, however due to time constraints the n-channel CCD47 was not tested. Results found using a CCD02 characterised using comparable voltages, timings, and X-ray flux [4] were used to provide the n-channel comparison. The X-ray method was selected as the measurement technique for CTI, using Mn-K α X-rays at 5,898 eV (~ 1600 e⁻), measured between -40.0 °C and -110.0 °C, with the dark current measured between 0.0 °C and -110.0 °C.

*jpdg3@open.ac.uk; phone +44 (0) 1908 852 769; fax +44 (0) 1908 858 052; www.open.ac.uk/cei

The CCD tested was the e2v technologies plc front illuminated CCD47-20, a frame transfer device with an image and store format of 1024 by 1024 with 13 μm square pixels, illustrated in Figure 1a. The parallel and serial buried channel widths are 8.5 μm and 24.0 μm respectively. The p-type buried channel was doped with boron, the epitaxial layer with phosphorous (20 to 100 $\Omega\cdot\text{cm}$), and the substrate with antimony ($< 20 \text{ m}\Omega\cdot\text{cm}$). The dopants were selected to provide comparable resistivity and properties to those found in n-channel devices, for ease of manufacture [5]. The concentration of phosphorous is two orders of magnitude lower than that in n-channel devices; therefore the formation of E-centre defects will be negligible [5]. The CCD02 is a front illuminated device, with an image format of 385 by 578 with 22 μm square pixels, illustrated in Figure 1b. The parallel and serial buried channel widths are 17.5 μm and 36.0 μm respectively.

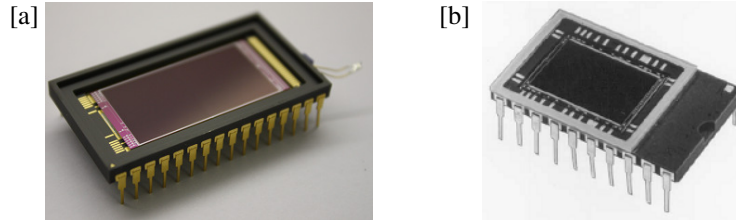


Fig. 1. A photograph of the p-channel CCD47-20 [a] and the n-channel CCD02 [b]

A proton irradiation was originally conducted, using two p-channel devices and one n-channel device, at the Kernfysisch Versneller Instituut (KVI) in the Netherlands. The image area was irradiated leaving the store region un-irradiated to act as a control, serial CTI would not be measured as the serial register was not irradiated. A pre-irradiation characterisation was not performed and post-irradiation it became apparent that the irradiated devices, and un-irradiated devices from the same wafer, exhibited defects which flooded the active area with excess charge. As a result testing moved to six p-channel devices which had been irradiated as part of an e2v study into p-channel and n-channel devices, funded by ESA. The entire active area of six p-channel devices and one n-channel device were irradiated using 63 MeV protons at the Paul Scherrer Institut (PSI) in Switzerland, with one n-channel and p-channel device held as a control. The irradiation details, including the 10 MeV proton fluence, is summarised in Table 1. Post irradiation an anneal stage at 100 $^{\circ}\text{C}$, with the irradiated devices unbiased, was performed for a duration of 168 hours the p-channel devices exhibited negligible change in CTI post anneal [5].

Table 1. Irradiation Characteristics for p-channel and n-channel CCD47-20s

<i>Device Type</i>	<i>Beam Energy (MeV)</i>	<i>Flux ($\text{p}\cdot\text{cm}^{-2}\cdot\text{s}^{-1}$)</i>	<i>Fluence ($\text{p}\cdot\text{cm}^{-2}$)</i>	<i>10 MeV equivalent fluence ($\text{p}\cdot\text{cm}^{-2}$)</i>
×3 p-channel	63	1.70×10^8	2.70×10^{11}	1.35×10^{11}
×3 p-channel	63	1.40×10^8	8.12×10^{10}	4.07×10^{10}
×1 p-channel	Not irradiated			
×1 n-channel	44	1.95×10^7	3.03×10^9	1.68×10^9
×1 n-channel	Not irradiated			

2. EXPERIMENTAL ARRANGEMENT

The CCD47 was housed inside the vacuum test facility shown in Figure 2. A vacuum pump was used to evacuate the air in the chamber with testing occurring at a pressure of $< 10^{-5}$ mbar. The CCD being tested was clamped onto a copper cold bench connected to a CryoTiger® refrigeration system (PT-30) capable of cooling the detector to around -120 $^{\circ}\text{C}$ or 153 K. A resistive heater was employed in thermal contact between the copper cold bench, allowing a maximum operating temperature of -40 $^{\circ}\text{C}$ before overloading the cooling capacity of the CryoTiger®. To allow for warmer operating temperatures the data were recorded as the CCD cooled, with the heater at maximum to reduce the cool down rate. The temperature can be controlled to within ± 0.1 $^{\circ}\text{C}$ using a feedback system, comprising a Lakeshore 325 temperature controller, platinum resistance thermometer (PRT), and the heater. The temperature of the CCD ceramic was

measured using a 1,000 Ω PRT (it is assumed the device silicon is in good thermal contact with the ceramic). An Oxford Instruments XTF5011/75-TH X-ray tube (tungsten anode) was used to fluoresce a manganese target held at 45° to the incident X-ray beam to provide a known energy (5,898 eV) for calibration and CTI measurements, with an X-ray density of approximately one event every two hundred and fifty pixels.

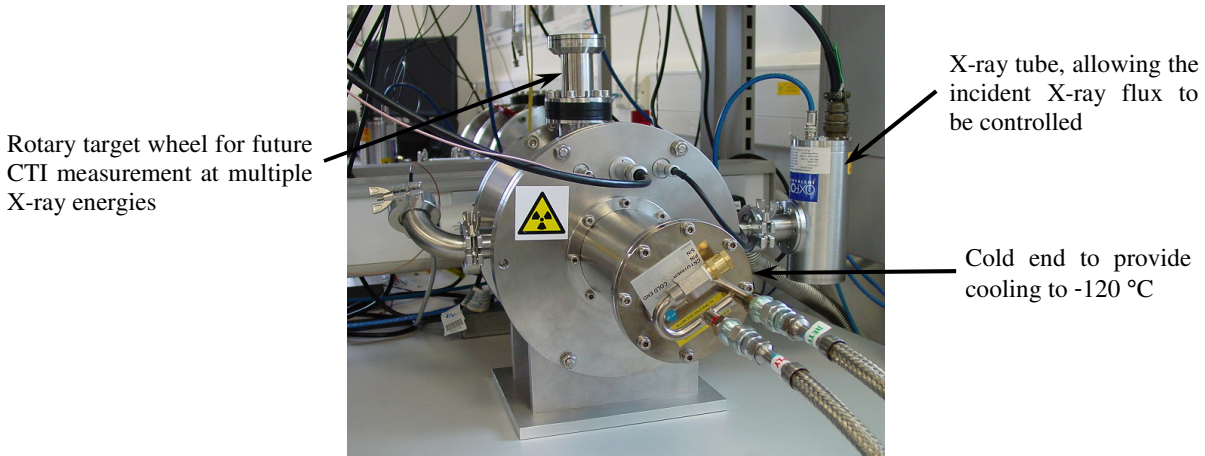


Fig. 2. A photograph of the vacuum test facility

Initially a potential mirror was created to convert the potentials provided by the XCAM Ltd. USB2REM1 camera drive box to those required to operate the p-channel CCD, given in Table 2. Mirroring the clock and reset potentials introduced a large amount of additional system noise, therefore, the mirror on the clock and reset potentials was removed and the ground referenced to 12.0 V to provide the required potentials. The total noise measured at -110 °C reduced from 200 e⁻ r.m.s. to 20 e⁻ r.m.s after the removal of the potential mirror. A headboard provided local low-pass filtering for the D.C. bias connections and pre-amplification of the output, with the clocking and biasing provided by an XCAM Ltd. USB2REM1 camera drive box in conjunction with USB2 v1.15 drive software. The devices were operated using a line transfer rate of 50 kHz, and a readout rate of 500 kHz.

Table 1. CCD47-20 operational voltages

<i>Clock/Bias</i>	<i>Description</i>	<i>Bias Used (V)</i>
V _{ss}	Substrate	0.0
V _{og}	Ouput gate	3.0
V _{rd}	Reset drain	17.0
V _{od}	Output drain	32.0
I \emptyset	Image/Store clock	12.0
R \emptyset	Register clock	12.0
\emptyset R	Reset gate	12.0
V _{ABD}	Anti blooming drain	28.0

3. RESULTS AND DISCUSSIONS

3.1 Dark Current

The mean dark current was measured across the surface of the p-channel devices using six sets of images, each taken using a 30 s integration period, the results as a function of temperature for three of the devices are shown in Figure 3. Srour demonstrated that a trap with an activation energy of 0.63 eV, attributed to the divacancy, is responsible for the temperature dependence of dark current associated with thermally generated charge [6]. The data should be proportional to $\exp(-0.63/kT)$, where k is Boltzmann's constant and T is the temperature. The data were plotted in an Arrhenius plot,

shown in Figure 4, with a line of best fit drawn through data points above $-55\text{ }^{\circ}\text{C}$. The feature formed below $-90\text{ }^{\circ}\text{C}$ is believed to show the limit of the measurement technique, where insufficient dark current is generated to be measured, requiring a longer integration period. The activation energy was calculated to be 0.61 eV un-irradiated, 0.62 eV irradiated with $4.07 \times 10^{10}\text{ protons.cm}^{-2}$, and 0.63 eV irradiated with $1.35 \times 10^{11}\text{ protons.cm}^{-2}$, the results are comparable to those found by Srour [6], Bebek *et. al.* [7], and Spratt [8]. This suggests that for the p-channel devices tested the divacancy is the dominant source of thermally generated dark current pre and post irradiation. The increase in dark current as a function of proton fluence is approximately linear. Based on the fits to the data the increase after irradiation at $21\text{ }^{\circ}\text{C}$ (at this temperature the device was saturated i.e. ADC max out) was calculated to be $\sim 1.4\text{ nA.cm}^{-2}\text{.krad}^{-1}$, similar to that found in the p-channel CCD02 [9] and other e2v n-channel CCDs [10].

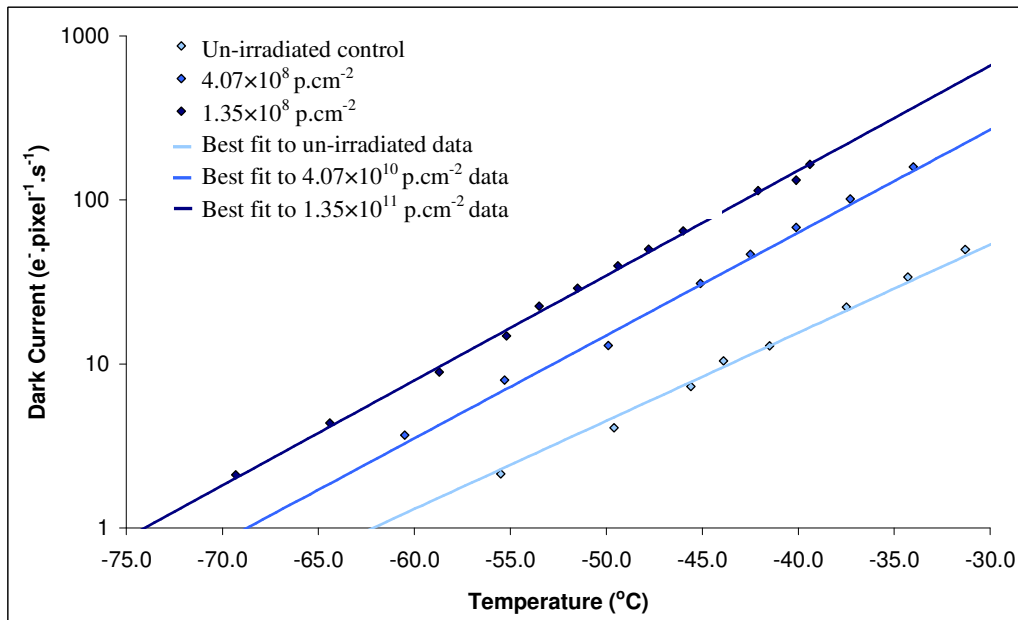


Fig. 3. Dark current as a function of temperature for three p-channel devices pre and post irradiation

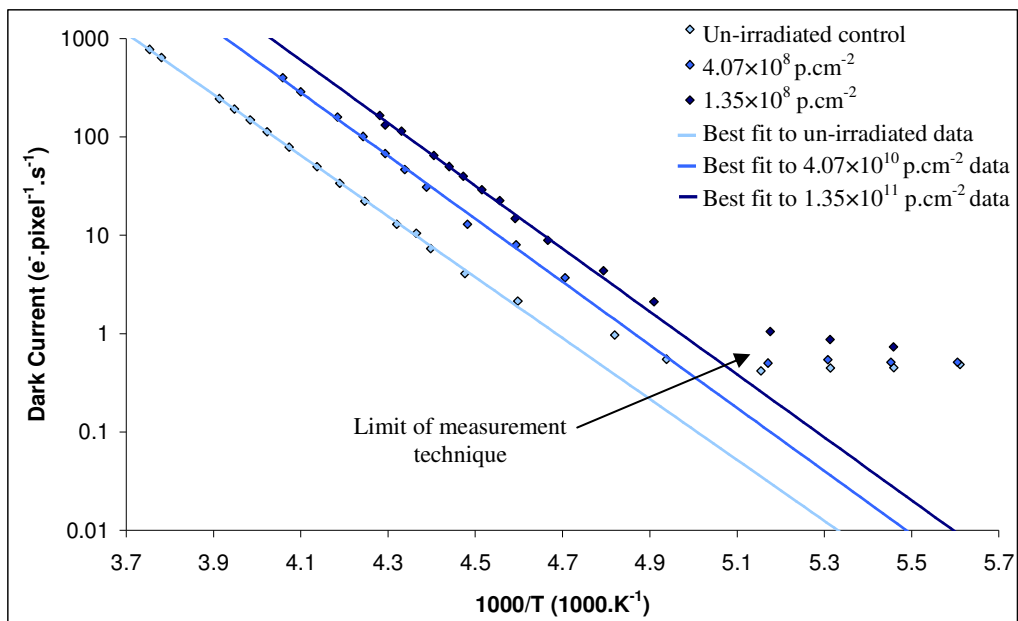


Fig. 4. Dark current as a function of $1000/T$ for three p-channel devices pre and post irradiation

3.2 Charge Transfer Inefficiency

The initial testing was performed using the p-channel control CCD held at -110.0 °C using an X-ray density of one event per 700 pixels, conducting fifteen readouts in 10 °C intervals, the results for parallel CTI are displayed in Figure 4. To increase the rate of data collection and the number of data points the X-ray density was increased to one event per 250 pixels, requiring only six readouts taken at 5 °C intervals, the results for parallel CTI are displayed in Figure 5. As expected there is a slight decrease in parallel and serial CTI, less than 3% and 11% at -90 °C respectively, as a result of the increased X-ray flux resulting in more traps remaining filled during readout. The decrease in CTI above -60 °C has been attributed to increased thermally generated dark current. Only the X-ray events detected within the store region were used in the CTI analysis, events from the image region were smeared over too many pixels.

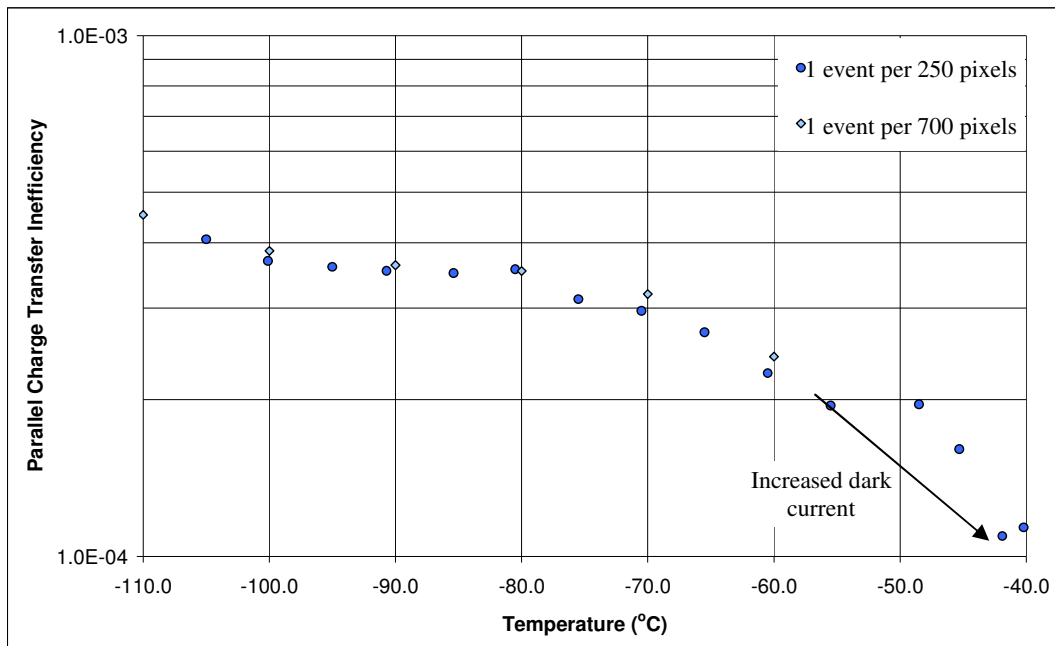


Fig. 5. Parallel CTI measured using the p-channel control as a function of temperature with different Mn-K α event densities

The CCDs which had been irradiated were then tested, due to the high CTI only the top 600 rows and first 800 columns were used in the CTI analysis. The temperature dependence of parallel CTI pre and post irradiation is shown in Figure 6, the trend for the irradiated and un-irradiated devices both demonstrate an increase in CTI as the device is cooled, possibly due to removal of thermally generated charge keeping the traps filled. Data were not taken, from the irradiated CCDs, above -45 °C due to the increased dark current making CTI analysis difficult.

The temperature dependence of serial CTI pre and post irradiation is shown in Figure 7, the trend shows an increase in CTI between ~-40 °C and ~-60 °C, attributed to thermally generated dark current, and between -60 °C and -110 °C a decrease, attributed to the increase in emission time in relation to the readout rate of 500 kHz. The slow parallel line transfer, at 50 kHz, does not benefit from the increased emission time. The p-channel CCDs tested exhibited comparable parallel CTI, however, the serial CTI varied between the un-irradiated device and devices irradiated with the same proton fluence, as illustrated in Figure 7 where the CTI of a CCD irradiated with 4.07×10^{10} protons.cm⁻² was measured to be lower than the un-irradiated control. Unfortunately the devices were not available for testing prior to the irradiation; it has been assumed that the effect is due to operational differences between the CCDs.

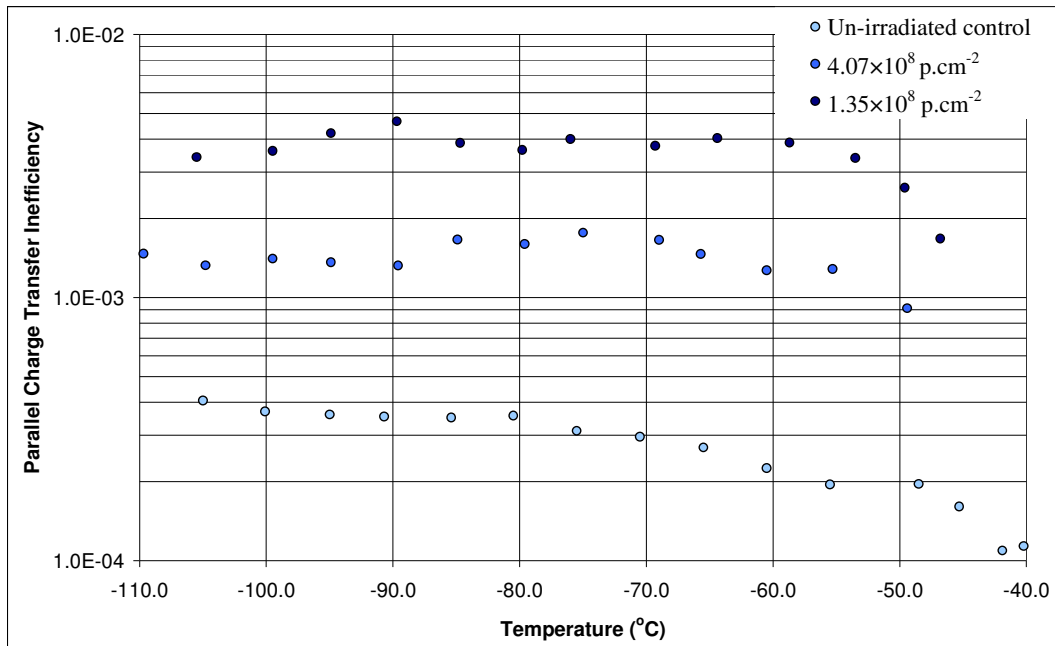


Fig. 6. Parallel CTI of the un-irradiated and irradiated p-channel devices as a function of temperature

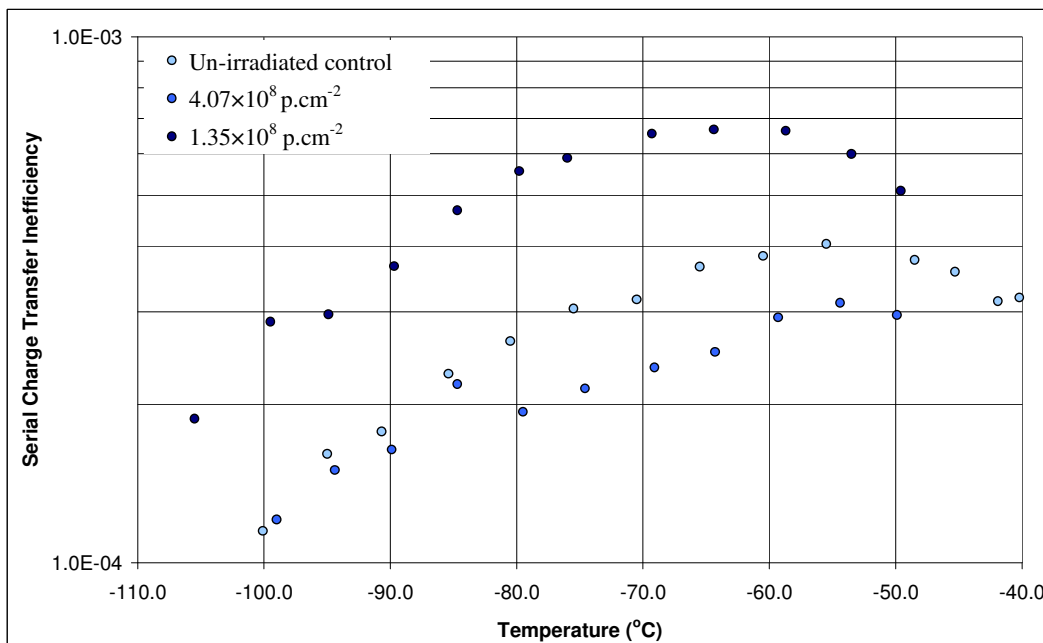


Fig. 7. Serial CTI of the un-irradiated and irradiated p-channel devices as a function of temperature

The parallel CTI measured at -90 °C is illustrated in Figure 8, with trend lines showing the base CTI pre-irradiation and the increase in CTI post-irradiation summed together to illustrate the effect of increased proton fluence on CTI at -90 °C. Data from an n-channel CCD02 [4] is included in Figure 9, the difference in the base CTI between these p-channel devices and a typical n-channel is clear. The function of increased CTI with proton fluence of the linear trend lines, the CTI damage constant, was compared to estimate the improvement in tolerance to radiation induced parallel CTI of the p-channel devices tested, an improvement of $\times 7$ was calculated for equivalent pixel geometries. Using the trend lines for

serial CTI and the same calculation method the improvement to radiation tolerance of serial CTI was found to be $\times 15$ for equivalent pixel geometries. It should be noted that the e2v test results at $-30\text{ }^{\circ}\text{C}$ and $-50\text{ }^{\circ}\text{C}$ only indicated an improvement of a factor >3 for radiation tolerance in serial CTI and less for parallel [5]. This highlights the importance of measuring the CTI effects over a range of temperatures due to changes in trap behaviour as a function of temperature, and when making comparisons between devices to use the same temperature.

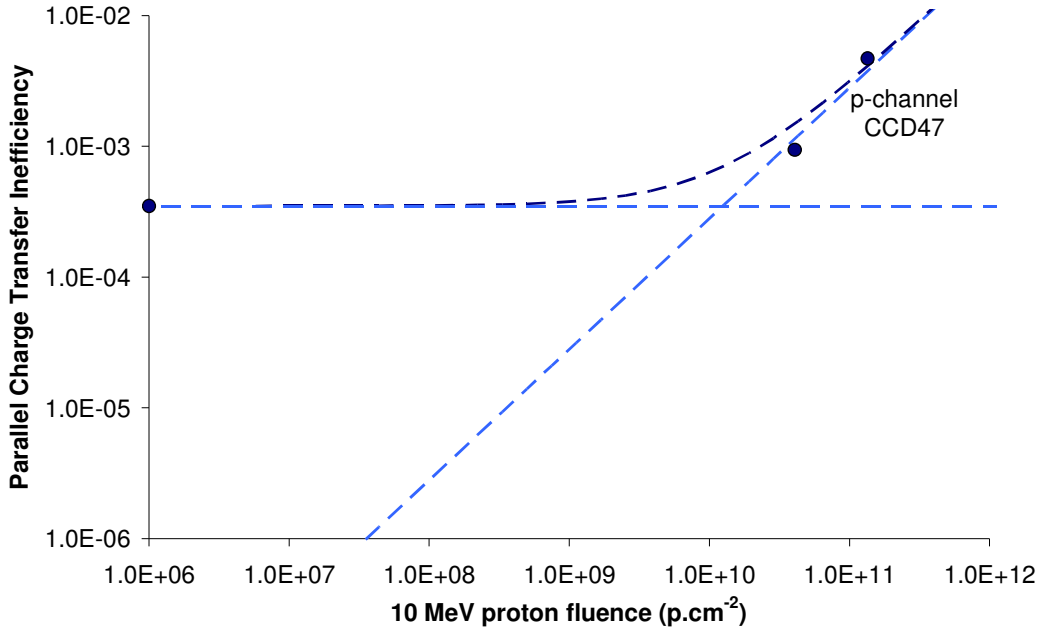


Fig. 8. Trend in parallel CTI at $-90\text{ }^{\circ}\text{C}$ based on the experimental data showing the base CTI and the effect of increased proton fluence

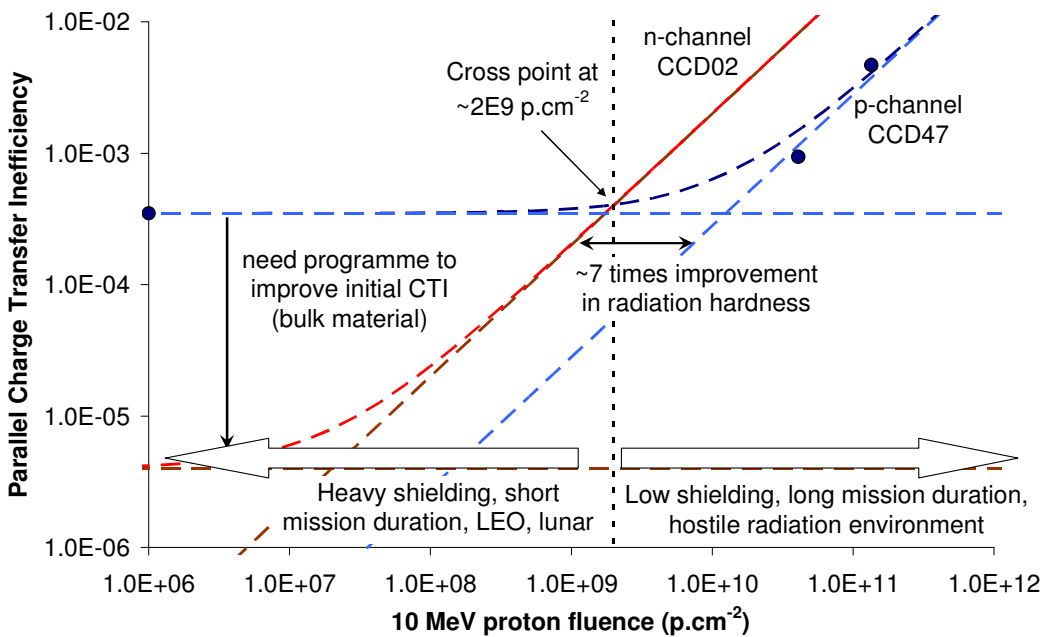


Fig. 9. Comparison of the p-channel CCD47 with an n-channel CCD02 at $-90\text{ }^{\circ}\text{C}$ showing the $\times 7$ improvement in radiation tolerance and the operational suggestions for a p-channel CCD47 at its current level of performance

4. CONCLUSIONS

The p-channel CCD47s tested demonstrate a clear improvement in tolerance to radiation induced CTI, showing an improvement of $\times 7$ and $\times 15$ for parallel and serial CTI respectively for equivalent pixel geometries when compared to an n-channel CCD. A program is required to improve the base parallel and serial CTI, possibly through the use of a bulk (float zone) devices which have demonstrated base CTI equivalent to n-channel devices, demonstrated by Bebek *et. al.* [7] and Dawson *et. al.* [11]. These devices, the CCD47s tested, would not be suitable for a space mission where the majority of the operational lifetime is spent below a 10 MeV equivalent proton fluence of $\sim 2 \times 10^9$ protons.cm⁻², as shown in Figure 9, i.e. missions that are heavily shielded, have a short mission duration, or are in a low Earth or lunar orbit. These devices would be suitable for a mission that expected to receive high proton fluence prior to the operational start of the instrument where the improved radiation tolerance outweighs the poor base CTI, i.e. missions that can only carry a low amount of shielding, have a long mission duration (Jupiter), or enter a hostile radiation environment (near solar).

The temperature dependence of thermally generated dark current exhibited a trend proportional to around $\exp(-0.63/kT)$ indicating that the divacancy is the dominant trap type both pre and post irradiation. The increase in dark current with proton fluence, measured to be ~ 1.4 nA.cm⁻².krad⁻¹ at 21 °C, was found to be comparable with other e2v n-channel CCDs [10]. Unfortunately the devices were not available for testing prior to the irradiation so no comparison could be made on the rate of hot pixel generation.

Future work will include completing the testing with the n-channel CCD47, measuring the parallel CTI as a function of temperature as only the n-channel device irradiated at KVI is available for testing. Some n-channel and p-channel high-Rho devices, which were also irradiated at KVI, are available for testing using the extended pixel edge response technique (the X-ray method is not suitable due to the low responsivity of the devices). The potential mirror will also be developed to improve its noise performance. Despite the initial poor CTI the large improvement in tolerance to radiation induced CTI still makes these devices, at their current level of performance, suitable for use in hostile radiation environments indicating that p-channel devices will have a large part to play in the future of CCDs in space.

REFERENCES

- [1] Stassinopoulos, E. G., Raymond, J. P., “*The Space Radiation Environment for Electronics*”, Proc. of the IEEE, vol. 76, pp. 1423-42, 1988
- [2] Spratt, J. P., Passenheim, B. C., Leadon, R. E., “*The Effects of Nuclear Radiation on P-channel CCD Imagers*”, IEEE Radiation effects data Workshop, pp. 116-121, 1997
- [3] Lumb, D. H., “*CCD radiation damage in ESA Cosmic Vision missions: assessment and mitigation*”, Proc. SPIE 7439 in press
- [4] Holmes-Siedle, A., Holland, A., Watts, S., “*The impact of space protons on X-ray sensing with charge with charge coupled devices (CCDs)*”, IEEE Trans. Nucl. Sci., vol. 43, no. 6, pp. 2998-3004, 1996
- [5] De Monte, B., Pool, P., Turton, J., Guyatt, N., King, R., “*Proton Irradiation Test – Summary Report*”, e2v internal report, 2008
- [6] Srour, J. R., “*Universal damage factor for radiation induced dark current in silicon devices*”, IEEE Trans. Nucl. Sci., vol. 47, no. 6, pp. 2451-2459, 2000
- [7] Bebek, C., Groom, S., Holland, S., *et. al.*, “*Proton Radiation Damage in P-channel CCDs Fabricated on High-Resistivity Silicon*”, IEEE Trans. Nucl. Sci., vol. 49, no. 3, pp. 1221-1225, 2002
- [8] Spratt, J. P., Passenheim, B. C., Leadon, R. E., “*The effects of nuclear radiation on P-channel CCD imagers*”, Proc. IEEE Radiation Effects Data Workshop (NSREC) Rec., Snowmass, 1997
- [9] Hopkinson, G. R., “*Proton Damage Effects on P-channel CCDs*”, IEEE Trans. Nucl. Sci., vol. 46, no. 6, pp. 1790-1796, 1999
- [10] Hopkinson, G. R., Dale, C. J., Marshall, P. W., “*Proton Effects in Charge-Coupled Devices*”, IEEE Trans. Nucl. Sci., vol. 43, no. 2, pp. 614-627, 1996
- [11] Dawson, K., Bebek, C., Emes, J., *et. al.*, “*Radiation Tolerance of Fully-Depleted P-Channel CCDs Designed for the SNAP Satellite*”, IEEE Trans. Nucl. Sci., vol. 55, no. 3, pp. 1725-1735, 2008